

Article

Building Capacity for a User-Centred Integrated Early Warning System for Drought in Papua New Guinea

Jessica Bhardwaj ^{1,2}, Yuriy Kuleshov ^{1,2,*}, Zhi-Weng Chua ^{1,2}, Andrew B. Watkins ¹, Sue Lynn Choy ² and Qian (Chayn) Sun ²

¹ Bureau of Meteorology, Docklands 3008, Australia; jessica.bhardwaj@bom.gov.au (J.B.); zhi-weng.chua@bom.gov.au (Z.-W.C.); andrew.watkins@bom.gov.au (A.B.W.)

² SPACE Research Centre, School of Science, Royal Melbourne Institute of Technology (RMIT) University, Melbourne 3000, Australia; suelynn.choy@rmit.edu.au (S.C.); chayn.sun@rmit.edu.au (Q.S.)

* Correspondence: yuriy.kuleshov@bom.gov.au; Tel.: +61-3-9669-4896

Abstract: Drought has significant impacts on the agricultural productivity and well-being of Pacific Island communities. In this study, a user-centred integrated early warning system (I-EWS) for drought was investigated for Papua New Guinea (PNG). The I-EWS combines satellite products (Standardised Precipitation Index and Vegetation Health Index) with seasonal probabilistic forecasting outputs (chance of exceeding median rainfall). Internationally accepted drought thresholds for each of these inputs are conditionally combined to trigger three drought early warning stages—“DROUGHT WATCH”, “DROUGHT ALERT” and “DROUGHT EMERGENCY”. The developed I-EWS for drought was used to examine the evolution of a strong El Niño-induced drought event in 2015 as well as a weaker La Niña-induced dry period in 2020. Examining the evolution of drought early warnings at a provincial level, it was found that tailored warning lead times of 3–5 months could have been possible for several impacted PNG provinces. These lead times would enable increasingly proactive drought responses with the potential for prioritised allocation of funds at a provincial level. The methodology utilised within this study uses inputs that are openly and freely available globally which indicates promising potential for adaptation of the developed user-centred I-EWS in other Pacific Island Countries that are vulnerable to drought.

Keywords: disaster risk reduction; early warning systems; Pacific Island Countries; Papua New Guinea; drought; satellite precipitation products; probabilistic climate forecasts

Citation: Bhardwaj, J.; Kuleshov, Y.; Chua, Z.-W.; Watkins, A.B.; Choy, S., Sun, Q. Building Capacity for a User Centred Integrated Early Warning System for Drought in Papua New Guinea. *Remote Sens.* **2021**, *13*, 3307. <https://doi.org/10.3390/rs13163307>

Academic Editors: Luca Brocca and Xianjun Hao

Received: 9 July 2021

Accepted: 18 August 2021

Published: 20 August 2021

Publisher's Note: MDPI stays neutral with regard to jurisdictional claims in published maps and institutional affiliations.



Copyright: © 2021 by the authors. Licensee MDPI, Basel, Switzerland. This article is an open access article distributed under the terms and conditions of the Creative Commons Attribution (CC BY) license (<http://creativecommons.org/licenses/by/4.0/>).

1. Introduction

Drought is a cumulative climatic phenomenon that has far reaching social and environmental impacts resulting from a precipitation deficit. There is no universal definition of drought that fits all purposes; instead, drought is often classified into the broad categories of meteorological, agricultural, hydrological and socioeconomic [1]. In this study, we examined drought holistically, with a particular focus on the combined impacts of agrometeorological drought which pertains to agricultural detriments resulting from meteorological rainfall deficiency.

The Pacific Island Countries (PICs) are composed of 15 heterogenous, diverse countries that occupy the region spanning 15°N to 23°S within the Western Pacific Ocean. Despite their varied physical, historical and climatological characteristics, PICs share common vulnerabilities such as small populations, significant habitation in low-lying coastal areas and fragile economies. This makes drought impacts particularly dire for the livelihoods of drought-vulnerable communities in these countries [2,3]. The 2020 World Risk Report found PICs such as Vanuatu, Tonga, the Solomon Islands and Papua New Guinea (PNG) to be in the top 15 most at risk to natural hazards such as drought [4].

In PNG, agrometeorological drought has significant impacts on subsistence agriculture, as over 80% of the population is estimated to be involved in subsistence agriculture and cash crops [5]. Tuber varieties such as sweet potato and yams are the dominant staple food group in PNG with over 60% of the rural population dependent on sweet potato as their main food source [6]. These characteristics make food production systems in PNG particularly exposed to collapse in times of drought. In 2015, El Niño-induced drought resulted in widespread food shortages when drought-related frosts caused subsistence crops to fail at a catastrophic scale. It was estimated that up to 2.4 million people were affected, and many perished from famine conditions [7].

Prolonged precipitation deficit periods are common throughout the history of PICs, with palaeoclimatological analysis of charcoal bands in fluvial sediments indicating the existence of such periods up to 5000 years ago [8]. However, due to anthropogenic climate change, droughts are projected to become more frequent and severe [9]. This trend will have significant ramifications for the already drought-vulnerable populations of PNG and other PICs [2]. In some cases, the negative economic impacts of such events could be comparable to the gross domestic product produced by some PICs [9]. Thus, as drought becomes more prevalent and extreme, drought responses need to be increasingly proactive in treating drought as a risk rather than a crisis [10,11].

An early warning system (EWS) for drought is one such proactive mechanism that can support local stakeholders and decision makers in taking proactive, evidence-based decisions. EWSs are structures used to monitor, predict and manage disasters across the world [12]. They are complex, adaptive systems composed of four fundamental components [13,14].

1. Risk knowledge—identification of the worst impacts and threats including a consolidated assessment of any exposures and vulnerabilities.
2. Monitoring and warning—the infrastructure that detects climate variabilities in the lead up to a disaster with a sound technical and scientific basis.
3. Communication and dissemination—the communication framework that ensures early warnings are delivered efficiently to vulnerable groups.
4. Response capability—the systems and knowledge that enable communities to effectively respond to early warnings.

An EWS that is user-centred and integrated within the broader disaster response network of a country has the potential to save lives, limit physical damage and lessen financial losses [15]. In this context, user-centred describes a system that is a strong, interconnected system that does not consider warning delivery to be linear or end-to-end, with a substantial focus on the users of the system [16,17].

However, a user-centred EWS alone may be futile in its construction if there is no consideration for the structural implementation of the system as one that is either centralised, decentralised or integrated. In this context, a centralised EWS is one that operates at a federal or state level [18] and interacts coarsely with a national audience, whereas a decentralised system operates on a finer scale with a more localised audience and tends to roll out warnings through established trust networks [18]. Centralised systems provide invaluable information on a coarse scale to government officials and management agencies. However, they are not so efficient in disseminating actionable, granular information to small-scale farmers, regional communities and the individuals most at risk [18–21]. Decentralised systems tend to do this well and have been found to generate extensive community involvement and trust in the system; however, the technical infrastructure for such systems is usually poor. In this way, an integrated EWS (I-EWS) combines the strengths of both decentralised and centralised EWSs, thus minimising the weaknesses resulting from utilising one structural approach in isolation.

Thus, an I-EWS is best conceptualised as a system that is supported and sustained by a national meteorological service but is controlled and managed on a local scale: likely

through a diverse extension network that comprises both climate experts and local stakeholders [17]. An iterative system such as this would also be open to adjustment through dynamic feedback loops that minimise bureaucracy at all possible stages and prioritise community feedback [16].

The methodologies used to construct a complex system such as this would need to be equally complex and adaptive. The construction would involve combining elements of both quantitative (i.e., defining system decision rules and thresholds, and rigorous error testing) and qualitative research methods (i.e., understanding the psycho-social nuances of the community the EWS would service) [12,18]. Whilst this study focuses on the quantitative aspects of EWS development in PNG, we have spent considerable time liaising with PNG stakeholders and the National Weather Service and intend to further engage users in our work.

Developing a user-centred I-EWS for drought is an integral part of activities under the Climate Risk and Early Warning Systems (CREWS) international initiative [22]. In this study, by applying the methodology of Bhardwaj et al. (2021) [23] developed for Australia's Northern Murray–Darling Basin, we build the capacity for a user-centred I-EWS for drought in PNG.

To ensure an I-EWS for drought is effective at detecting periods of drought, there needs to be significant consideration for the system's inputs. There are over 150 drought indices that can be used to track the onset, evolution and cessation of drought [24]. The application of a certain type of index is dependent on the data availability, demographic needs and climatic conditions of a drought-vulnerable region [24]. In small island developing states and least developed countries, rain gauges and other in situ instruments for meteorological observations are often limited in spatial density and long-term infrastructural maintenance. For PNG, this means that, despite a total land area of around 462,840 km², there are only seven operational rain gauge stations [22]. For comparison, the Australian region of south-east Queensland alone has over 315 rain gauges for a 28,371 km² region [25]. Beyond spatial and infrastructural limitations, rain gauges are also prone to precipitation loss errors from wind, evaporation, wetting or splashing effects [26].

Satellite remote sensing datasets offer a cost-effective solution to such spatial and infrastructural limits as they provide data that have global high-resolution spatial coverage and are produced by credible national space and weather agencies. Consequently, there have been several studies across PNG and the Asia-Pacific region more broadly that have sought to analyse the accuracy of satellite remote sensing datasets [27–30]. Such remote sensing studies have sought to determine the meteorological and agricultural indices best suited to detecting drought, with several further using artificial neural networks to generate deterministic and statistical forecasts of such indices [31–33]. Whilst such statistical methods have shown promising accuracy, they are still critiqued for their use of deterministic prediction models that do not incorporate degrees of randomness as a meteorological or climatological probabilistic forecast or hydrological model would [34].

A promising input for the inclusion of probabilistic forecasting into a drought I-EWS would be the sub-seasonal to seasonal forecasts generated by national meteorological agencies [35]. Such forecasts are already operational and are routinely updated to continuously improve forecasting skill. Some studies have explored the potential of seasonal forecasting for drought prediction, but few studies have explored the coupling of such probabilistic outputs with observational satellite remote sensing products [35,36]. This gap in the literature of combined observational and predictive products informs the selection of inputs used in this study and further allows warnings to be staged by concern and action level. Simplistically, drought concern should be highest when dry conditions are both observed and forecasted compared to if wet conditions are observed but dry conditions are forecasted.

2. Materials and Methods

2.1. Study Area

Papua New Guinea is a large island country with around 9 million inhabitants and an estimated 851 different spoken languages [37]. PNG has vast highlands, tropical forests and over 600 small islets and atolls which makes it home to an estimated seven percent of the world's biodiversity [38]. At the sub-national scale, PNG is divided into 22 provinces which are depicted in the topographical map (Figure 1). This map was created in QGIS using topography data from ETOPO2v2 [39].

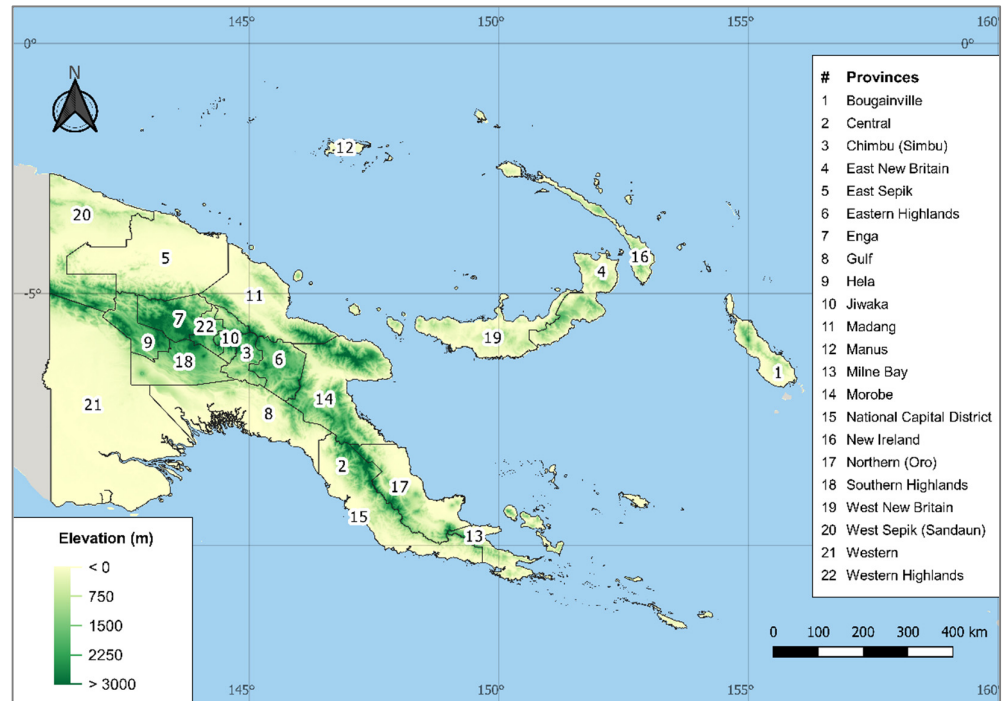


Figure 1. Topographical map of the study area with the 22 provinces of PNG displayed using a numbered key.

The PNG Highlands are a notable feature—reaching a maximum elevation of 4509 metres above sea level and providing diverse ecosystems and agricultural potential [40]. It is estimated that 75% of PNG's annual sweet potato production is grown in the Highlands, making it an agriculturally important region for the country [6,41]. Despite this, there are limited meteorological observations for the Highlands [42]—likely due to the region's remoteness. The Highlands also have complex impacts on the country's climatology. The climate of most of PNG is essentially tropical with some monsoonal influence from the West Pacific Monsoon [43,44]. However, the Highlands experience meteorological phenomena that differentiate them from the low-lying parts of the country [43]. This results in little to no seasonality over parts of the Highlands, compared to the somewhat distinctive rainfall seasonality of the low-lying regions [44,45].

2.2. Drought I-EWS Inputs

The inputs selected for the monitoring component include the Standardised Precipitation Index (SPI) and the Vegetation Health Index (VHI). The chance of exceeding median rainfall (CEMR), as generated by a probabilistic forecasting model, is an input for the forecasting component of the I-EWS. These inputs were selected due to their promising performance in several drought detection studies in the Asia-Pacific region [46–48] and, most importantly, for their noteworthy performance in a drought detection study over PNG

conducted by Chua et al. (2020) [30].

2.3. Input Thresholds

The SPI and VHI inputs are commonly used to analyse drought evolution, escalation and dissipation and thus have internationally accepted thresholds that can be used to indicate periods of precipitation and vegetation state anomalies [49,50]. In this study, we accompanied these with the CEMR to include a predictive component. Each input, its relevant equations, timescales, primary references and thresholds used for drought detection are presented in Table 1.

Table 1. Drought I-EWS inputs—relevant equations, timescales and drought thresholds.

Input	Relevant Equations	Timescale	Drought Threshold	Available Time Range	Native Resolution
Standardised Precipitation Index [49]	$SPI = \frac{p - p_m}{\sigma}$ <p>where p—precipitation over a certain time period, p_m—mean rainfall over the same period, and σ—standard deviation over the same period.</p>	3-month standardisation	SPI-3 < -1 indicates mild to extreme drought	2000 to now	0.1° (~10 km)
Vegetation Health Index [50]	<p>The VHI is a weighted combination of the Vegetation Condition Index (VCI) and the Temperature Condition Index (TCI). VCI and TCI are derived from the Normalised Difference Vegetation Index (NDVI) and Brightness (radiative) Temperature (BT), respectively.</p> $VCI = 100 \cdot \frac{NDVI - NDVI_{min}}{NDVI_{max} - NDVI_{min}}$ $TCI = 100 \cdot \frac{BT_{max} - BT}{BT_{max} - BT_{min}}$ $VHI = \alpha \cdot VCI + (1 - \alpha) \cdot TCI$ <p>where α is the weighted coefficient that combines VCI and TCI; most of the literature assigns $\alpha = 0.5$.</p>	3-month accumulation	VHI-3 < 40 indicates mild to extreme drought	2013 to now	0.1° (~10 km)
Chance of Exceeding Median Rainfall [51,52]	ECMWF's CEMR is generated from a complex dynamic climate prediction model that uses a range of initial conditions and evolves them for 50 ensemble members.	1-month forecast conditions projected	CEMR-1 < 40% indicates low chance of exceeding median rainfall for the next month	2015 to now	O640 (~18 km)

These selected inputs were temporally limited in their availability which restricted the beginning of the study period to January 2015.

For this study, SPI and VHI data were obtained through the World Meteorological Organisation's (WMO's) Space-based Weather and Climate Extreme Monitoring (SWCEM) products [53]. Further SPI data were obtained from the Multi-Source Weighted-Ensemble Precipitation (MSWEP) dataset [54]. WMO SWCEM provides access to satellite precipitation estimates and derived products from the USA National Oceanic and Atmospheric Administration's (NOAA's) Climate Prediction Center (CPC) and the Japan Aerospace Exploration Agency (JAXA). We used 3-month SPI and VHI, which are both calculated on a moving 3-month window, for example, March SPI-3 and VHI-3 use January–March rainfall and NDVI and BT data, respectively.

Evaluating the accuracy of WMO SWCEM satellite precipitation estimates, Chua et al. (2020) [30] identified JAXA's satellite precipitation product, the Global Satellite Mapping of Precipitation technique (GSMaP) [55,56], as the best performing over PNG compared to CMORPH satellite precipitation products produced by the NOAA/CPC. Chua et

al. (2020) [30] further identified that VHI was able to reliably capture the spatial and temporal aspects of a severe drought period in PNG.

Based on the findings of Chua et al. (2020) [30], the GSMaP-derived SPI was selected as the input into the monitoring component of the I-EWS for drought. However, in this study, we also examined the MSWEP-derived SPI given recent reports of its notable performance in the Pacific [54]. It is out of the scope of this study to evaluate and validate the performance of this dataset in comparison to GSMaP data, but nonetheless, we compared GSMaP and MSWEP SPI timeseries to analyse dataset implications and accuracy for drought detection using the developed I-EWS.

The predictive input for the drought I-EWS was seasonal to sub-seasonal (S2S) forecasts from the European Centre for Medium-Range Weather Forecasts (ECMWF) [51]. The ECMWF is one of the world's leading global weather and climate forecast-producing centres, with high-accuracy forecasts issued frequently.

The inputs selected for this study—the SPI, VHI and CEMR—were downloaded as raw gridded NetCDF datasets. The SPI, VHI and CEMR for each 0.10° grid cell over PNG were then extracted and averaged both nationally and across PNG's 22 provinces. This allowed us to deem the input variability between a national and a provincial scale and thus indicate whether this system should be downscaled to a provincial level.

2.4. Decision Rules

The selected inputs were then combined to form thresholds of drought warning that fall under escalating categories of “DROUGHT WATCH”, “DROUGHT ALERT” and “DROUGHT EMERGENCY”. The decision rules for each warning category are presented in Figure 2 and accompanied with a qualitative description.

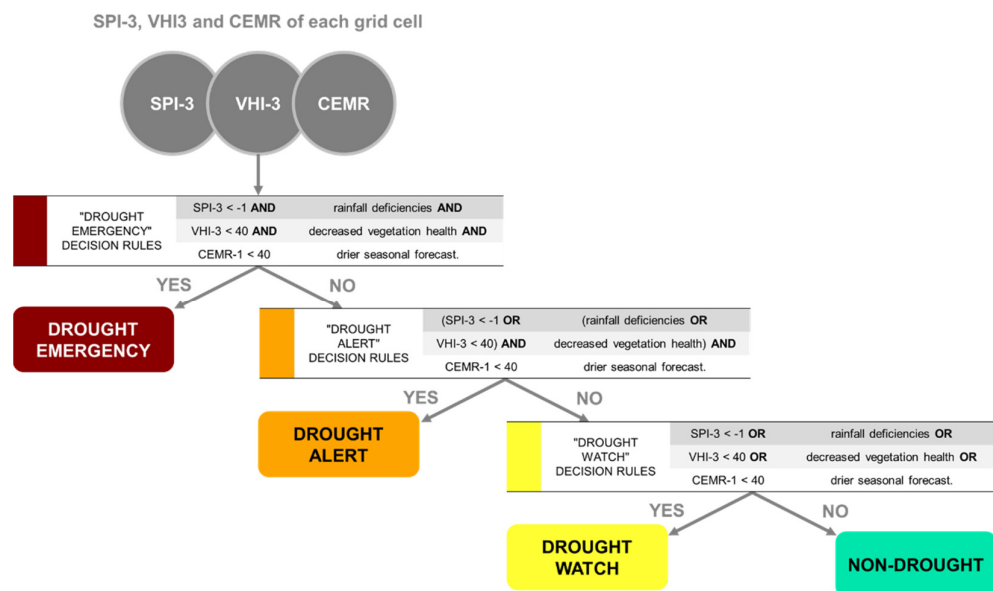


Figure 2. Drought I-EWS decision rule process.

To generate the drought alert level, the SPI, VHI and CEMR inputs are masked over the ocean and interpolated to a 0.10° resolution. Then, the SPI, VHI and CEMR values for each 0.10° grid cell within PNG are passed through the decision rules. A raw gridded file, a plotted file and a provincial status file are outputted. The gridded file contains raw NetCDF data which are then plotted using the Matplotlib plotting library. This plotted file indicates the drought warning level of each grid cell in PNG in visual form. The provincial status file is a comma-separated value (.csv) file that detects the overall drought warning level for each province in PNG. The overall status is determined by an algorithm

that counts the occurrence of each WATCH, ALERT and EMERGENCY grid cell in a province and selects the modal warning level to be the overall provincial status. In the case where more than one mode is detected, the highest urgency mode is selected. A diagram indicating this described workflow that produces warnings from these decision rules is provided in Figure 3.

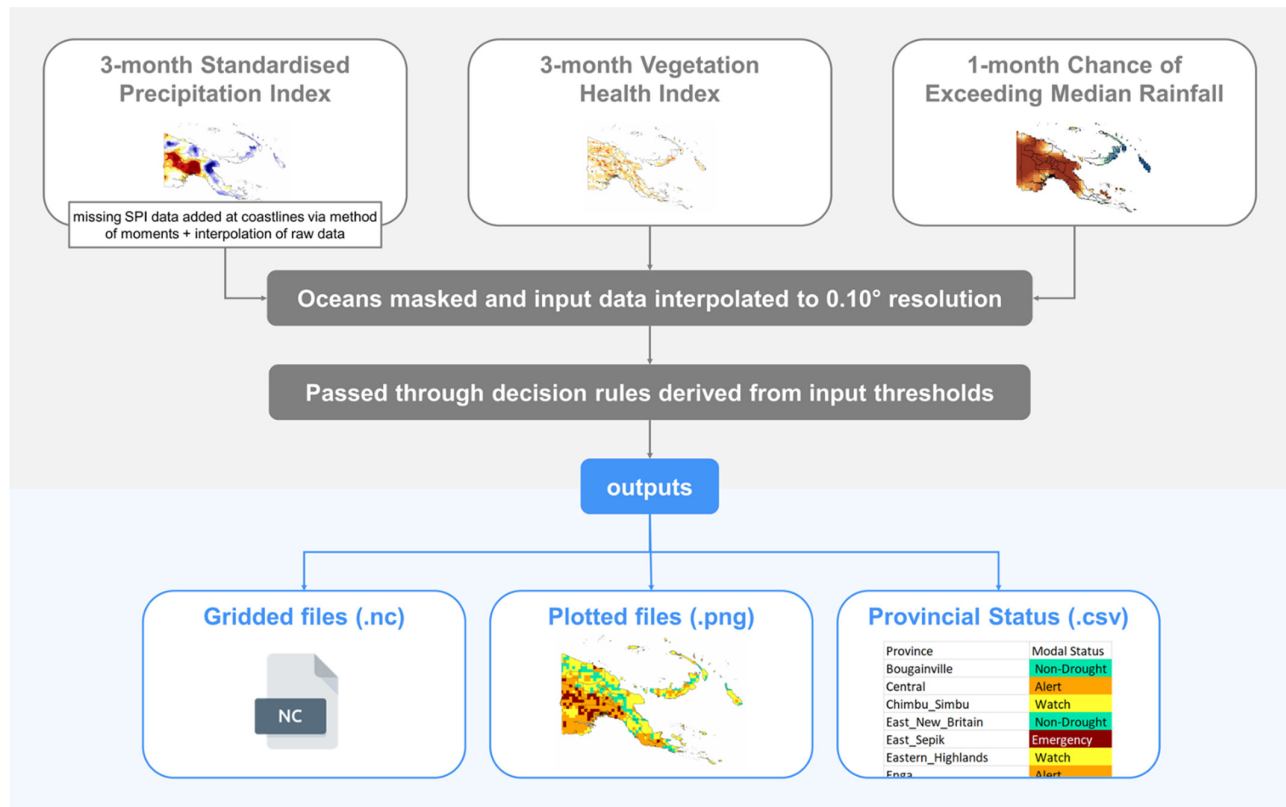


Figure 3. Workflow diagram of the drought I-EWS in this study.

Drought grids, maps and status summaries were generated for the temporal period of overlap between all datasets. Periods of heightened drought risk were then analysed in detail for the possible lead time of the drought warning provided.

Throughout this study, the authors worked closely with the PNG National Weather Service and prospective drought I-EWS stakeholders. Two CREWS-PNG stakeholder workshops were held in November 2020 and May 2021 to introduce the results of this research and its implications. This also created a forum to open a dialogue and gather feedback from stakeholders and users.

3. Results

To first visualise the evolution of I-EWS inputs, timeseries of all three inputs were generated over the study period (January 2015–April 2021). These timeseries are depicted in Figures 4–6. The black dotted line indicates the drought threshold for the respective input.

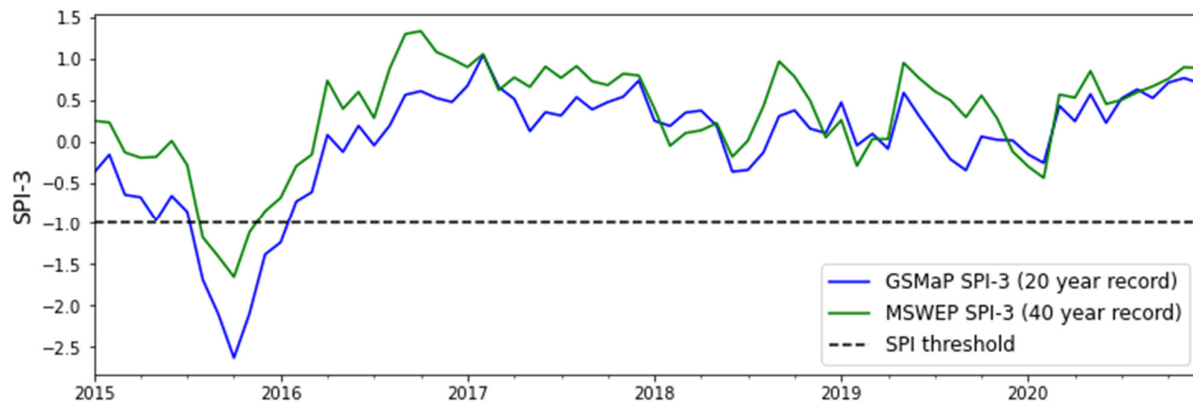


Figure 4. Three-month Standardised Precipitation Index averaged over PNG from 2015 to 2020 for the two datasets analysed in this study—GSMaP and MSWEP.

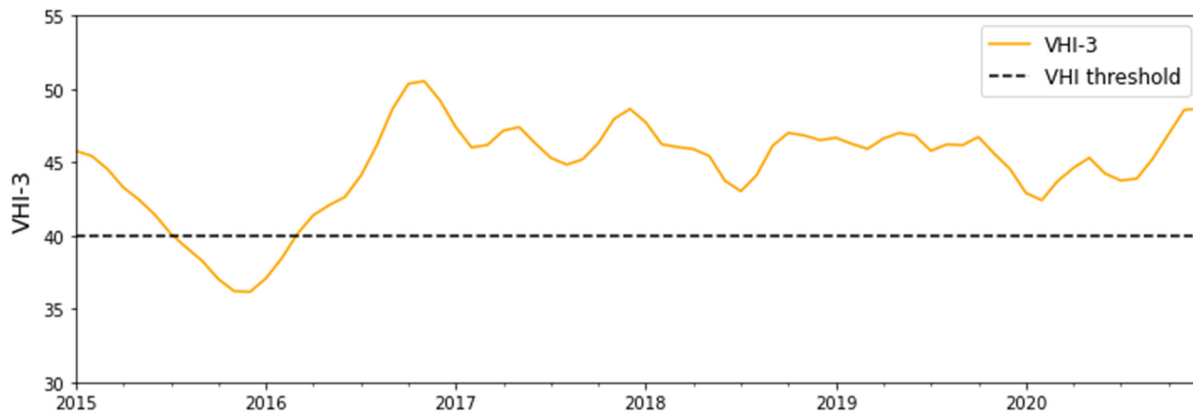


Figure 5. Three-month Vegetation Health Index averaged over PNG from 2015 to 2020.

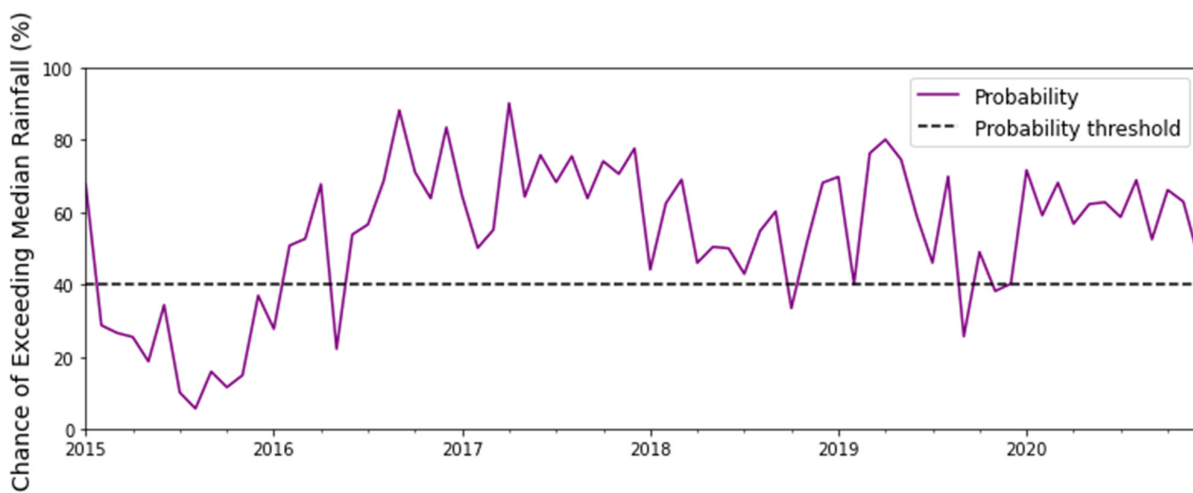


Figure 6. Chance of exceeding median rainfall probability averaged over PNG from 2015 to 2020.

There are evident synergies between Figures 4–6—with a strong dry signal detected throughout 2015. The mean, median and standard deviation of the nationally averaged SPI, VHI and CEMR datasets for the study period (January 2015–April 2021) are provided in Table 2.

Table 2. Mean, median and standard deviation for nationally averaged SPI-3, VHI-3 and CEMR-1 for the month ahead.

	Input	National Mean	National Median	National Standard Deviation
SPI-3	GSMaP	−0.01	0.18	0.72
	MSWEP	0.31	0.47	0.62
	VHI-3	44.75	45.68	3.21
	CEMR-1	53.80	57.72	19.85

The means, medians and standard deviations provide insight into the spread of the data, and all inputs have means and medians above their respective thresholds (SPI = −1, VHI = 40 and CEMR = 40). This indicates that the inputs spend most of their time in “non-drought” conditions which is what would be realistically expected. However, GSMaP SPI and MSWEP SPI differ in their central tendencies—with GSMaP experiencing a slightly negatively biased mean compared to MSWEP’s positively biased mean. This is likely because GSMaP SPI uses a 20-year record beginning in 2000 compared to MSWEP’s 40-year record. In this shorter 20-year record, PNG experienced significantly negative SPI values in 2015–2016 when the country experienced a severe El Niño [7]. Since SPI values are standardised over a particular period, the occurrence of extremely negative SPI events over a relatively shorter record has the potential to lead to a more negative central tendency. The median is less severely affected by outliers which is likely why the GSMaP median is less negative over the same period (it is, in fact, positive). MSWEP’s SPI, on the other hand, is observed to experience a more positive mean and median which indicates the possibility of a positive bias in the dataset. Future research may choose to finetune SPI thresholds according to a decile or percentile analysis given that our findings indicate that PNG’s SPI “baseline” is non-zero. However, for the purposes of this study, we use the globally accepted −1 threshold and choose to use the MSWEP-derived SPI in preference to the GSMaP-derived SPI purely due to its longer precipitation record.

3.1. Analyses at Provincial Level

Timeseries analysis on a provincial scale was conducted to examine how the provincial data spread may vary from the national data spread. Significant variability between provincially and nationally averaged timeseries of SPI, VHI and CEMR is evident (see Figures 7–9, respectively). Further details on the mean, median and standard deviation of input data for each province can be found in Appendix A Tables A1–A3, respectively.

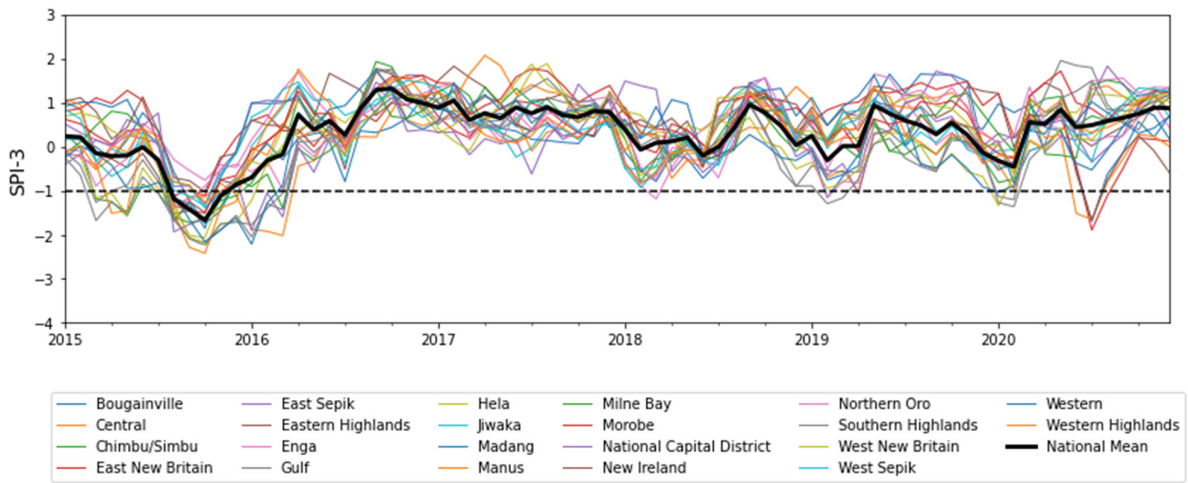


Figure 7. SPI-3 averaged over 22 PNG provinces from 2015 to 2020 and compared to the national mean (in bold black).

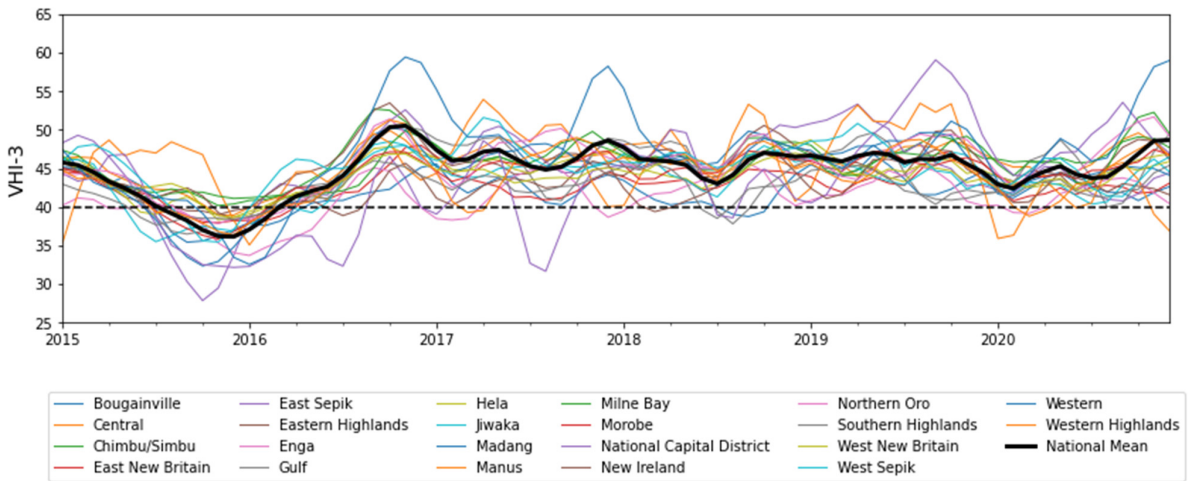


Figure 8. VHI-3 averaged over 22 PNG provinces from 2015 to 2020 and compared to the national mean (in bold black).

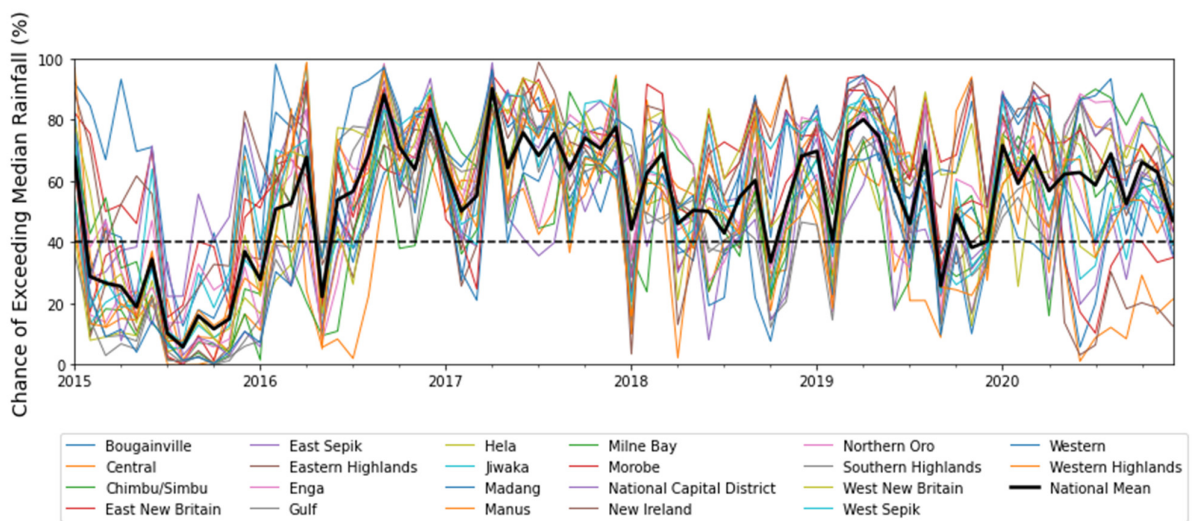


Figure 9. Chance of exceeding median rainfall for the next month averaged over 22 PNG provinces from 2015 to 2020 and compared to the national mean (in bold black).

The significant variation in the means, medians and standard deviations provides insight into the complex nature of PNG's climate and highlights the importance of observing drought on a provincial scale as opposed to a national scale. Thus, for this reason, the I-EWS scoped in this research downscales warning outputs to a provincial level. Given that disaster management in PNG is similarly relayed to Provincial Disaster Committees [38], this decision will be practical for the effective management and mobilisation of resources. Downscaling beyond the provincial level (such as to districts or local-level government areas) would incur significant computational costs, and the resolution of the underlying data is unlikely to be able to reflect the precision depicted by these scales. Given these considerations, we maintain a provincially scaled I-EWS analysis.

3.2. Drought Evolution

By applying the decision rules described in Section 2.4, spatio-temporal analysis of drought early warning for PNG over the study period was conducted, and the resultant maps and summaries were generated. An example of a drought warning map (September 2015 and May 2016 experimental product) is provided in Figure 10. A stacked area chart that depicts the proportion of grid cells in each drought warning category for all of PNG is provided in Figure 11. A detailed summary of the drought warning levels for each PNG province throughout the study period is presented in Figure 12.

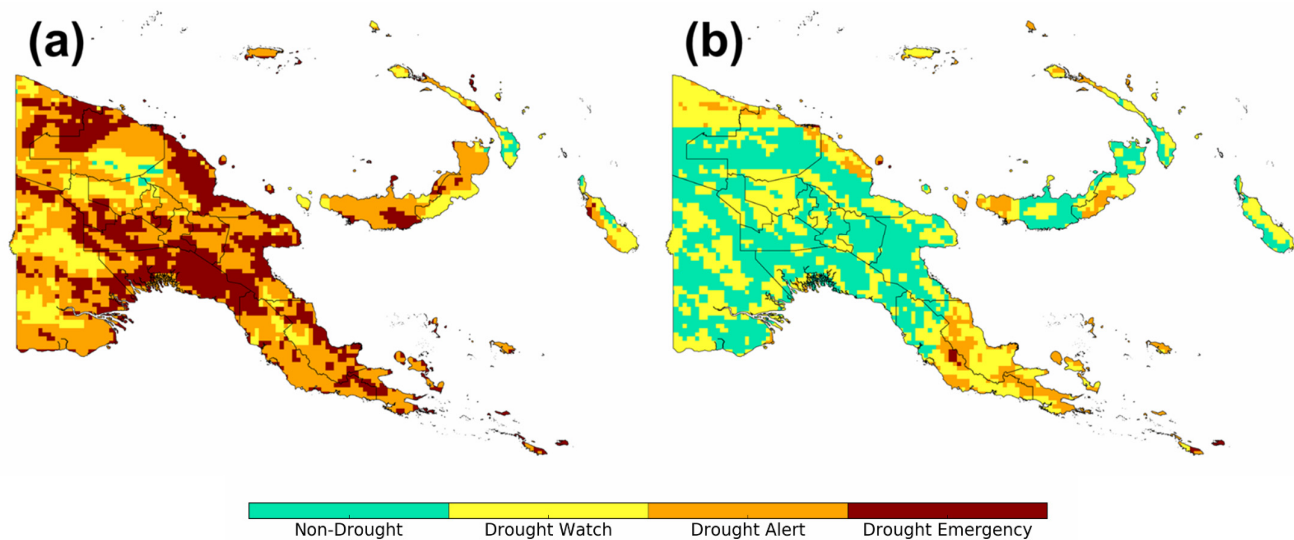


Figure 10. Drought warning maps for (a) September 2015 and (b) May 2016 (experimental product).

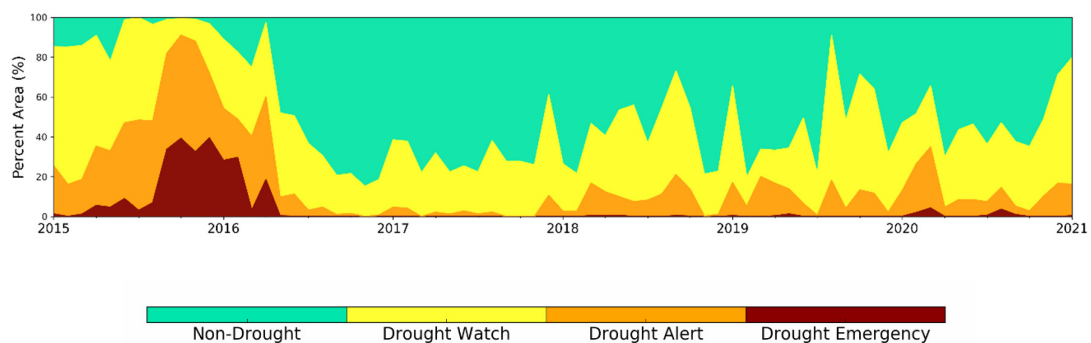


Figure 11. Drought warning stacked area chart over the study period.

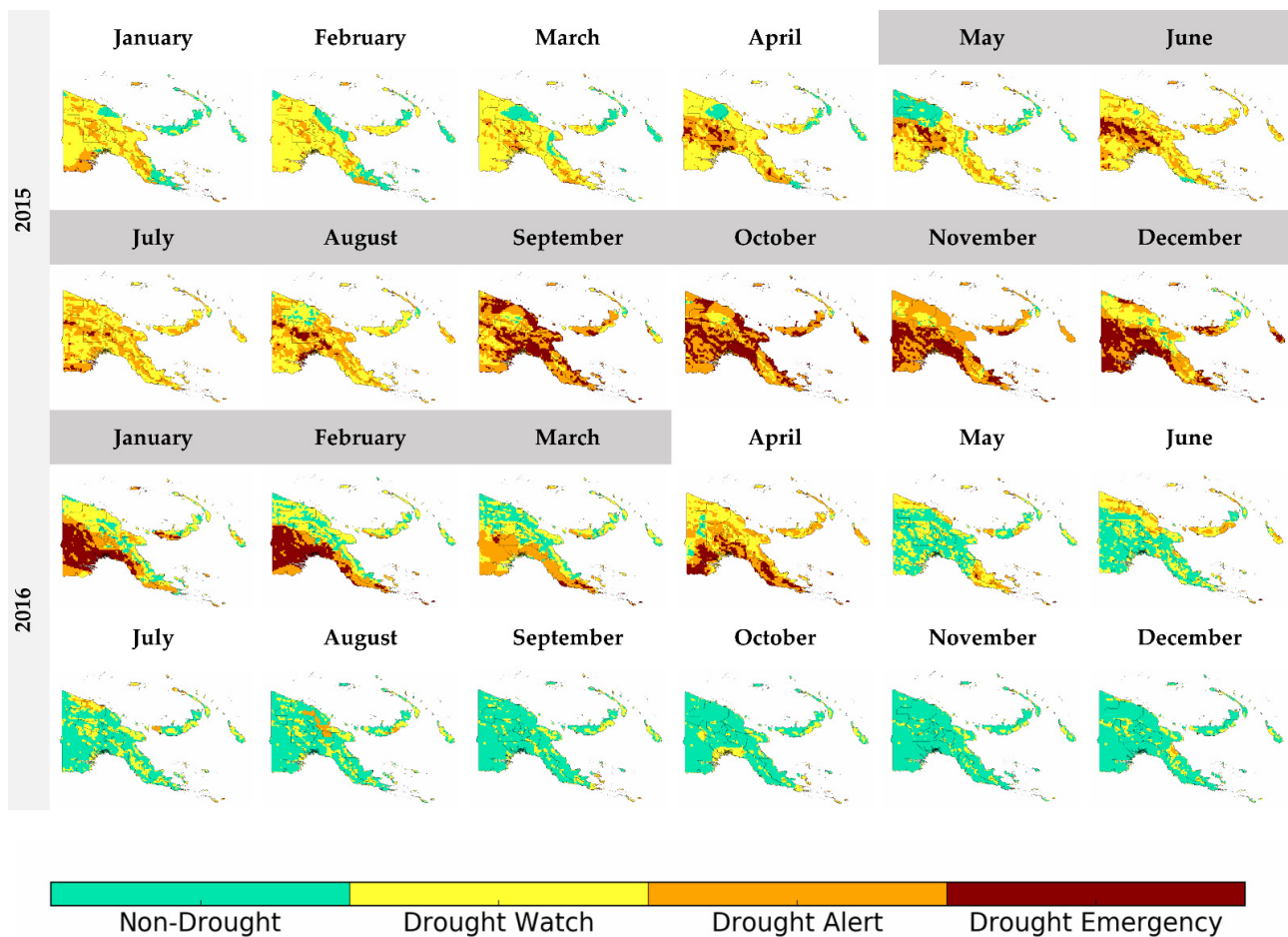


Figure 13. Drought I-EWS evolution of the 2015–2016 El Niño-induced drought in PNG. Dark grey bar indicates months when the El Niño was active as declared by the Bureau of Meteorology [57].

Historical analysis shows that El Niño and La Niña events impact Western Pacific rainfall in varying degrees [44]. In analysing rainfall data over PNG, Smith et al. (2013) [44] found the southern PNG mainland to exhibit a linear wetting and drying pattern from La Niña and El Niño, respectively; on the other hand, it was noted that PNG’s north-eastern islands and some Highland regions exhibit non-linear negative rainfall anomalies in both positive and negative El Niño Southern Oscillation (ENSO) events. There is even significant fluctuation in rainfall variation depending on the time of year an ENSO event occurs as well as the type of El Niño that develops—a Cold Tongue El Niño has been found to have a lesser drying effect in the north-east than a mixed or Warm Pool El Niño [58].

MSWEP rainfall data from 1980 to 2021 were examined—with years stratified according to La Niña and El Niño years according to the Bureau of Meteorology’s declaration of such years [57]. We plot rainfall deciles in all La Niña and El Niño years compared to climatology for the base period 1980–2020 in Figure 14a,b, respectively. This analysis method was also conducted over Australia and was found to be consistent with the Bureau of Meteorology’s analysis of ENSO-impacted rainfall for Australia [59,60], confirming its validity over PNG. The results indicate a negative rainfall anomaly over the mainland in El Niño years and a positive rainfall anomaly south of the PNG Highlands associated with La Niña—with the strongest anomaly signal over Western Province. In line with the findings of Smith et al. (2013) [44], the analysis indicates a tendency towards dry conditions over the New Guinea islands in both ENSO warm and cold events, with La Niña

conditions having a stronger drying effect.

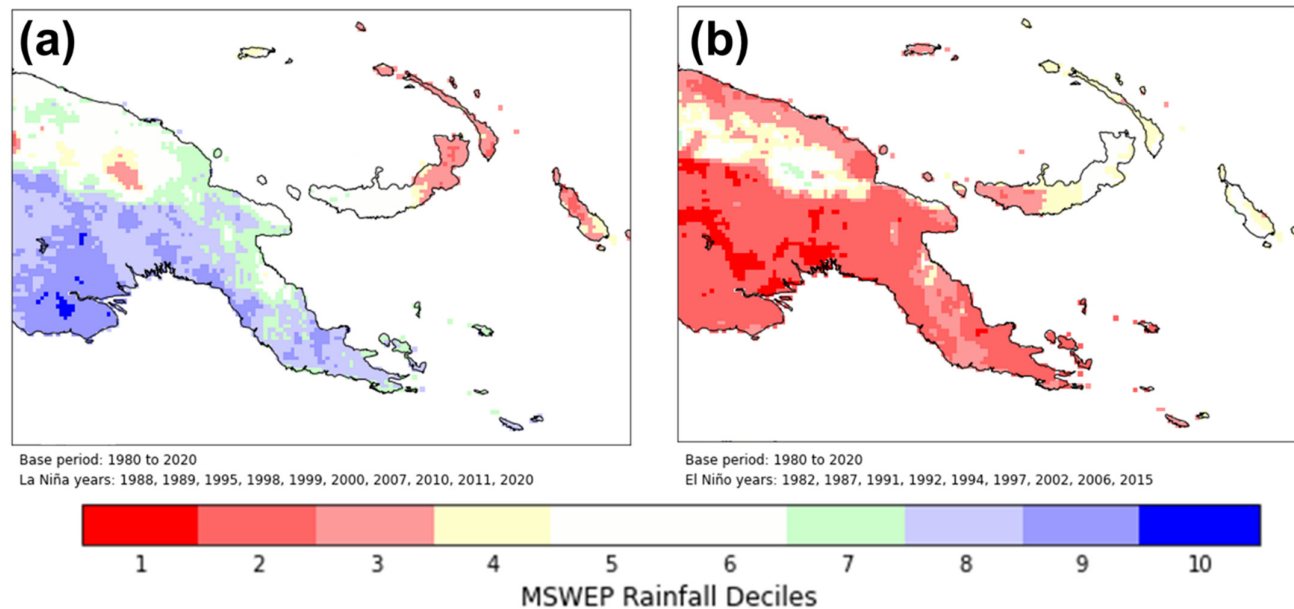


Figure 14. MSWEP rainfall deciles in (a) La Niña and (b) El Niño events compared to a base period of 1980–2020.

Despite this conceptually simple ENSO-related variation in rainfall, it is important to note that year-to-year rainfall variability in PNG is also impacted by other Pacific and Indian Ocean climate drivers, e.g., Indian Ocean Dipole (IOD). These influences can interact with ENSO impacts to weaken or exacerbate the reported tendency in the inter-annual rainfall variability. In Figure 15, we compute the MSWEP rainfall deciles in the (a) Negative and (b) Positive IOD years as declared by the Bureau of Meteorology [61]. This IOD analysis was conducted over austral winter and spring months as at other times of the year, annual rainfall in the region is dominated by monsoonal impacts and thus does not accurately reflect IOD impacts alone. We further investigate how the interaction of both Indian Ocean and Pacific Ocean climate drivers exacerbates each other's impacts in combined (c) Negative IOD and La Niña years and (d) Positive IOD and El Niño years [62]. Years where ENSO and IOD are inactive are deemed climatologically “neutral” in this analysis, and a plot of decile values in such years is provided in Appendix A Figure A1.

Of note is the exacerbated positive and negative rainfall extremes in concurrent Pacific and Indian Ocean events. In Negative and Positive IOD years, positive and negative rainfall biases are observed, albeit at a reduced intensity compared to the biases observed in the La Niña and El Niño years. However, in the combined IOD and ENSO events, rainfall impacts are extreme, with the New Guinea islands exhibiting a stronger negative rainfall bias than in the La Niña or Negative IOD years alone.

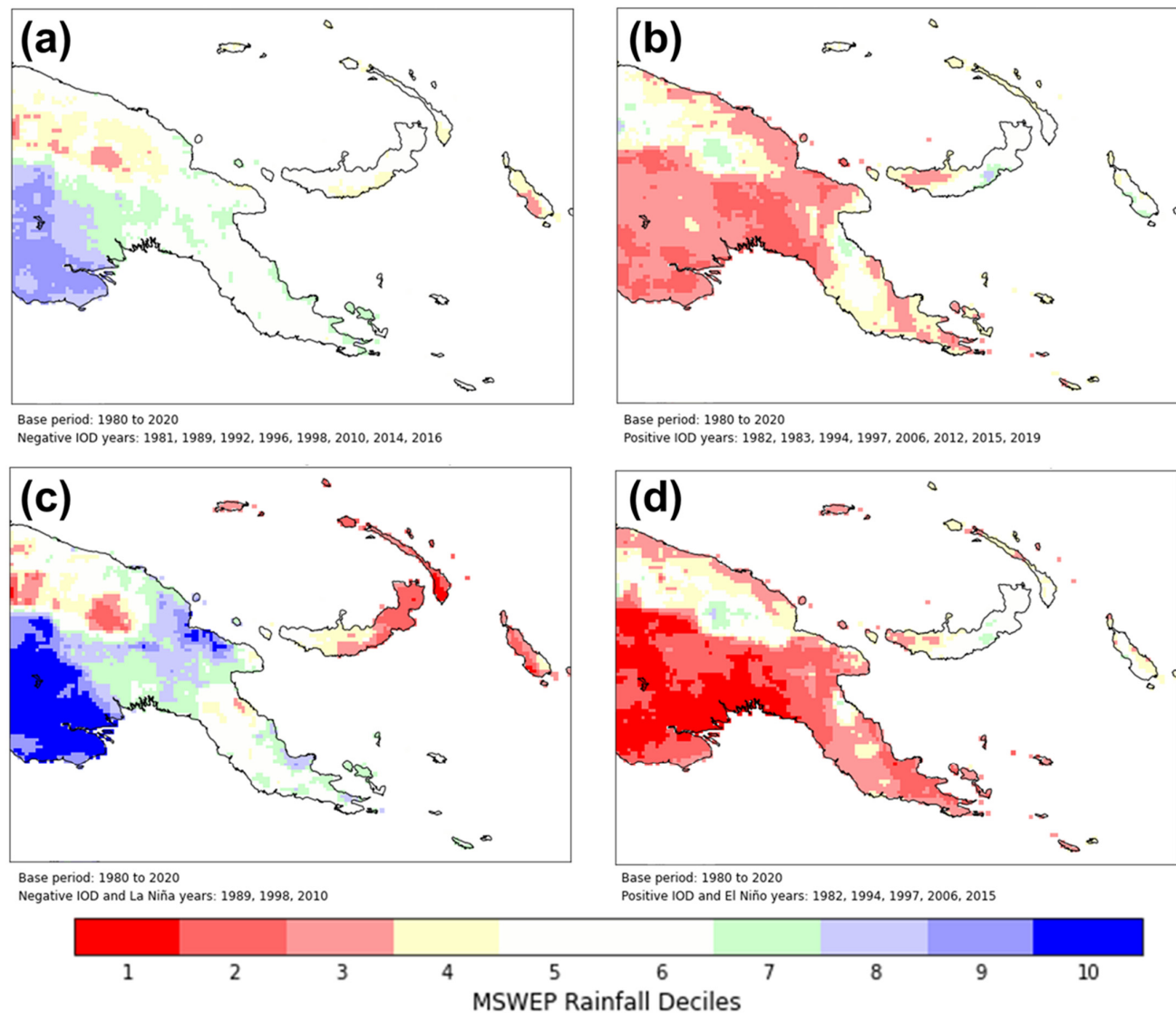


Figure 15. MSWEP rainfall deciles in (a) Negative IOD, (b) Positive IOD, (c) Negative IOD and La Niña and (d) Positive IOD and El Niño events compared to a base period of 1980–2020.

Another important observation is that 2015 was a combined El Niño and Positive IOD year. It is evident that both these climate drivers in tandem led to devastating negative rainfall anomalies with the induced drying trend observed in Figure 13, with the southern mainland showing a strong dry signal. The combined 2015–2016 El Niño and Positive IOD event was notably strong and thus impacted the whole nation, but stronger dry impacts can be observed over southern PNG—particularly as El Niño weakened in January of 2016 where southern PNG provinces are the last to remain in ALERT and EMERGENCY conditions (Figure 13). A WATCH similarly begins to develop over large parts of the southern mainland—with the New Guinea islands in the north-east being the last to enter drought conditions.

Aside from the stark dry period observed in late 2015, one other dry event is detected by the I-EWS that is the weaker dry period of late 2020 and early 2021. This period coincides with a La Niña event. As depicted in Figure 14, historically, dry conditions in north-eastern PNG are associated with both El Niño and La Niña impacts. The evolution of the dry conditions associated with the 2020–2021 La Niña is presented in Figure 16.

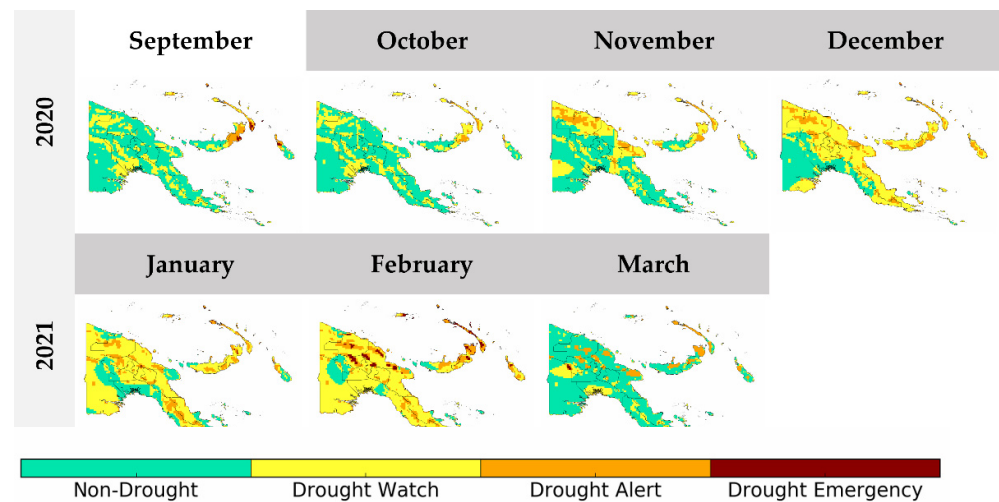


Figure 16. Drought I-EWS evolution of the 2020 La Niña-induced dry period in PNG. Dark grey bar indicates months when the La Niña was active as declared by the Bureau of Meteorology [57].

The weak dry event is evidently detected over the country, with the first provinces to enter DROUGHT WATCH being New Ireland, East and West New Britain, Bougainville and Manus in the north-east of the nation. These New Guinea islands are also the last to recover from this dry period, with significant March rainfall weakening their drought status but not reducing it to non-drought conditions. This drought event was relatively weak with no impacts reported in the literature to date. In this examined case, the warning lead time is around two months as dry conditions intensified in February 2021 and November and December 2020 were the first months that DROUGHT WATCHES became widespread. However, in a case such as this, the warning lead time is not as important as the system's ability to maintain a heightened yet weak status. Overall, the presented case studies demonstrate that the developed I-EWS has potential for detecting both weak and strong dry events.

4. Discussion

4.1. System Limited by Spatial Resolution of Inputs

For the purposes of this study, the drought I-EWS was interpolated to the finest resolution of the inputs' native resolutions. This was 0.1° (~10 km) for the SPI and VHI. This resolution is finer than the native resolution of CEMR which has a native resolution of O640 (~18 km). This means that the resolution of the I-EWS is restricted by the resolution of the inputs. This is particularly problematic for small provinces such as the National Capital District, which has only one interpolated 0.1° grid cell within its domain. This results in the National Capital District having a heightened drought warning status compared to the other larger provinces (Figure 12). Any variability in that one grid cell will thus bias the variability of the whole province. This is starkly contrasted to all the provinces in PNG which have an average of 29 grid cells within their domain, with a maximum of 138 grid cells in Western Province. Having more samples per province provides a more accurate and robust representation of the data, reducing the effects of outliers in the domain. To address this, it is recommended for space-based data providers (NOAA/CPC, JAXA, etc.) to aspire towards issuing finer native resolutions for the SPI and VHI where possible. For PNG, this only affects one province, but for smaller island states in the West Pacific, this spatial resolution would greatly impact the overall I-EWS performance.

4.2. Dataset Temporal Availability

For this study, we chose to use the MSWEP-derived SPI in preference to the GSMaP SPI due to its longer temporal range of data availability and promising performance in the West Pacific [54]. However, we recognise that each precipitation dataset has its deficiencies resulting from how it blends gauge data, the accuracy of algorithmic inputs and its performance over orography and in the tropics [63]. Since the SPI is a normalised precipitation index, we assume 0 to be equivalent to “normal” conditions. However, this is not always the case over the tropics. Deo (2011) [64] performed a Mann–Kendall test to identify significant SPI trends in Fiji and found that most stations indicated negative values, depicting dry conditions in both the Northern and the Western Divisions. The study further concluded that the temporally limited range of satellite datasets can limit drought diagnosis and detection through the SPI alone. In attempt to address this, we included other drought indices such as the VHI which are independent of the SPI and, when combined with escalating negative SPI values, can provide a somewhat holistic observation of evolving dry conditions. Future studies may further address SPI drought detection limitations by not assuming SPI = 0 to be the baseline of “normal” conditions and may instead use statistical machine learning approaches to determine an appropriate non-zero SPI threshold for “normal” and “dry” conditions. Additionally, there may also be scope for a decile-based SPI threshold, where, instead of using SPI = -1 as a drought threshold (corresponding to the lowest 15% of precipitation records), an SPI threshold of SPI = -1.28 may be preferred (corresponding to the lowest 10% of precipitation records) [49]. Both decile and machine learning methods would require significant further research over Papua New Guinea.

4.3. Minimising Rapid State Transitions

Maintaining users’ trust in the system is key in ensuring the system’s warnings are actionable. To avoid wavering trust, it is important to minimise rapid drought state escalations and de-escalations—especially when such state transitions jump or skip warning levels (i.e., “WATCH” to “EMERGENCY” or “ALERT” to “NON-DROUGHT”). Minimising such transitions can be addressed in two fundamental ways: through automation or through climate expert discretion. Automation minimisations may be achieved by introducing effective entry and exit points for each state (e.g., the watch entry rule is as described in Table 2, but to exit a watch status, consecutive days without rain must be above a certain number of days). Alternatively, or perhaps even in tandem, expert discretion from the prospective national weather service issuing warnings would also be critical in minimising rapid state transitions. Currently, the drought status for a given province is determined on a modal basis where the majority status of grid cells in a province determines the overall province status and, in the case of equivalent modes, the system chooses the highest alert level. However, this relatively arbitrary decision between two equally high modal states could be conducted by a climatologist in the PNG National Weather Service. To illustrate what this may look like, Figure 12 has been modified, and the results with grey squares to indicate months where equally high modal states were detected are presented in Figure 17. In cases such as these, experts could use their knowledge and on-ground reports to create smooth drought state transitions. For example, consider East New Britain (row 4) in July of 2015. In Figure 12, East New Britain jumps from a “WATCH” in June to an “ALERT” in July and then back to a “WATCH” in August as there is an equal number of grid cells in both “WATCH” and “ALERT” in July. A climatologist having background information about equally high modal statuses, as presented in Figure 17, may consult East New Britain’s Provincial Disaster Committee for on-ground drought reports and choose to maintain East New Britain’s “WATCH” status in July to minimise status wavering.

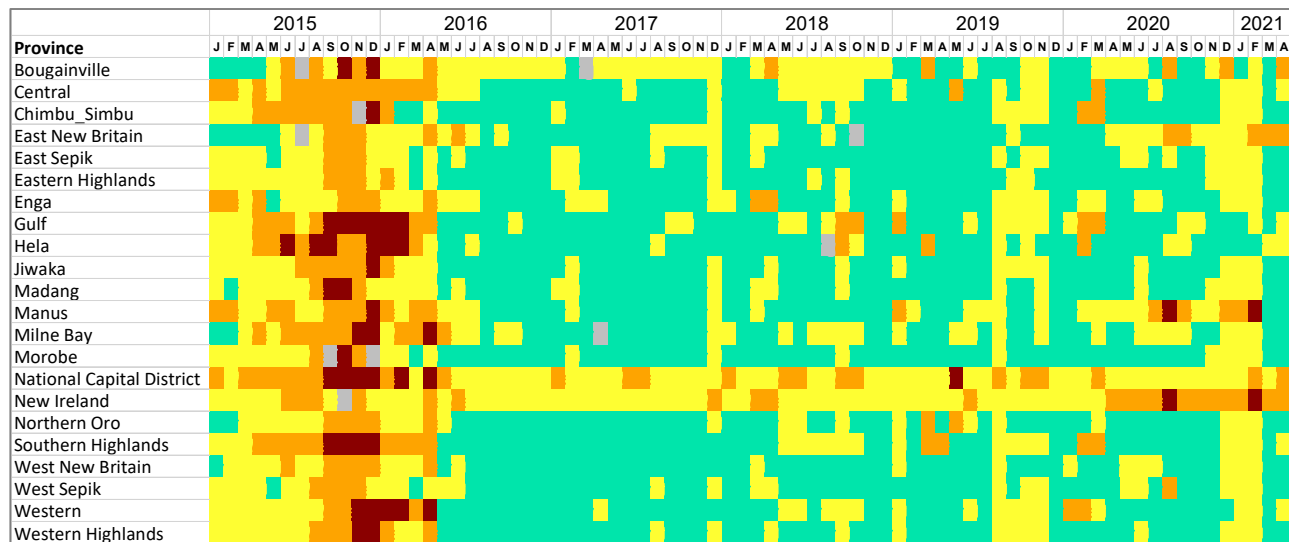


Figure 17. Same as Figure 12 but for months with equally high modal statuses indicated in grey.

Such user-centred expert discretion will be key in maintaining system trust, but we caution that it may need to be accompanied with careful standard operating procedures [16,65].

4.4. False Alarms and Success Rates

To further quantify the efficiency of such an I-EWS for drought, there needs to be significant validation of the initial results and insights. Future research in progressing this I-EWS intends to analyse the hit and miss rates of drought early warning—this requires the use of an independent variable for validation. Several remote sensing drought index studies used the SPI or VHI itself to verify the results of their drought findings; however, that would be inappropriate for this study as both indices are direct inputs into the system [66,67]. Ji et al. (2018) [68] faced a similar issue in their study and used crop yield as an “independent variable” against which to analyse drought detection. They acknowledged that even though crop yield is affected by several other extraneous variables, it was still the best option available for their research given it was removed from the direct inputs of their analysis. A similar proxy may be used for PNG depending on data availability—given that most agriculture in PNG is subsistence in nature, staple crop yield may be more appropriate. This could be interesting for PNG given that drought poses significant threats to the nation’s food security and is often the tipping point in the lead up to a food shortage crisis [69]. Such future verification should attempt to use robust mathematical verification processes such as hit and false alarm rate analysis and is the focus of our upcoming validation study [66,70].

4.5. Soil Moisture

The I-EWS for drought scoped in this study evaluates more than just meteorological drought through its consideration of both precipitation and vegetation conditions. However, the agrometeorological nature of this I-EWS could be further strengthened with the explicit inclusion of soil moisture (SM). For this study, SM inclusion was limited by a lack of robust SM satellite measurements or water balance models for PNG [71]. In their drought detection study over PNG, Chua et al. (2020) [30] further identified that SM satellite detection is likely to be difficult over PNG given its vast dense tropical rainforests and their interference with SM satellite retrieval mechanisms. Not having explicit SM inclusion may be a current limitation of this research; however, a study by Halwatura et al. (2017) [48] found that the SPI itself may be effective at detecting soil moisture deficiencies

over Australia. These results cannot directly be applied to PNG; however, we considered them in our decision to incorporate the 90-day SPI in preference to the 30-day SPI as it is widely acknowledged that the latter is not able to capture seasonal agrometeorological deficits as the longer-period SPI is able to [72].

4.6. Translating Warnings to Impacts

Throughout the I-EWS development process, stakeholder discussions highlighted the need for translation of warnings into actionable impacts. This is an area of growing complexity in disaster risk reduction efforts and is widely acknowledged to be crucial towards long-term EWS success [12]. Historically, the communication and dissemination of early warnings are identified within the literature as a general weakness of EWS design and implementation globally [65]. This is particularly problematic in PICs where EWSs may require a robust scientific and technical background that may not be communicated impactfully and in ways that align and complement existing traditional knowledge. The literature identifies numerous examples when such limitations in both early warning and seasonal climate forecast communication have led to significant misunderstandings within local communities. A study by Andersson et al. (2019) [19] investigated the barriers of seasonal forecast information uptake in South Africa’s Limpopo Province. The study highlighted the impacts of information misunderstandings whereby one participant mistook a 40% probability of rain with an expectation of 40 mm of rainfall. This indicated the importance of probabilistic information being issued with some impactful or educational context to illustrate what may eventuate for users when a 40% probability of rain is issued. In the case of EWSs, such conclusions are directly relevant to the usability and the actionability of warnings. If users cannot place warnings in the context of their livelihoods, then the EWS is ultimately futile in its efficacy. Concurrent research has sought to identify the determinants of actionability for EWSs in PICs and found several key factors conducive to successful early warning communication. These findings are listed in Table 3.

Table 3. Determinants of actionable early warning communication in Pacific Island Countries as identified by a literature review.

Determinants of Actionable Early Warning Communication		
Trust	Gender-Specific Inclusions	Traditional Knowledge Inclusions
<ul style="list-style-type: none"> ▪ Trust in warnings directly affects actionability [73]. ▪ Cognitive, emotional and organisational trust have differing impacts on risk perception [74]. ▪ Medium of warning communication affects trust placed in warnings’ actionability [73]. ▪ Mediums used for warning communication need to be diverse and must minimise population “blind spots”, i.e., those without mobile phones or radios [75]. ▪ Language of warning affects accessibility and actionability [76] 	<ul style="list-style-type: none"> ▪ Gender-based divisions are prevalent in Pacific Island societies [77]. ▪ Women have been identified to be unique and trusted disseminators of response and recovery in times of disaster [78]. ▪ In PNG, women undertake 80% of subsistence agriculture, making their inclusion vital from a food security perspective [79]. ▪ Aipira et al. (2017) highlighted several priorities for successful inclusion [80]. ▪ It is prefaced that any such inclusion in future research should not further burden existing gender divisions [78,80]. 	<ul style="list-style-type: none"> ▪ Traditional knowledge is commonly used by Pacific Island communities to prepare and respond to disaster [81–83]. ▪ In the face of climate change where disasters will be more frequent, this knowledge needs to be further integrated with scientific knowledge. ▪ Such inclusions ensure that disaster responses focus on cultural continuity and not acculturating aid [84]. ▪ There are few studies that explicitly investigate the scientific and traditional knowledge integration process. ▪ The work of Mercer et al. (2010) is formative in this field [84].

Our research team continues to place emphasis on such complementary qualitative I-EWS research, and we encourage future research to similarly investigate translating quantified warnings into qualitative impacts that communities can trust and understand.

5. Conclusions

This study presented a proof of concept of an agrometeorological drought I-EWS for PNG that pairs satellite remote sensing data with outputs from probabilistic forecasting models. The SPI, VHI and CEMR were combined as monitoring and forecasting components of an EWS. Thresholds and decision rules were defined from these inputs to trigger early warnings for three distinct stages—“DROUGHT WATCH”, “DROUGHT ALERT” and “DROUGHT EMERGENCY”. Furthermore, downscaling drought early warning to a provincial level provides warning granularity that would otherwise be missed at the national level. The evolution of the I-EWS through 2015 to 2021 was examined, and it was found that significant early warning for drought is possible 3–5 months in advance. The lead time detected by this I-EWS indicates the significance of a window of action and highlights how proactive action could be operationalised and enabled in a systematic way. We conclude that the developed I-EWS demonstrated an ability to detect both strong and weak drought events, and this study illustrates the promising potential for its operational implementation over PNG. However, such a system would need further iteration, verification and community engagement prior to operationalisation. The system’s conceptually simple design and its openly sourced satellite and forecasting inputs provide a valuable proof of concept for use in other drought-vulnerable countries in the Asia-Pacific region.

Author Contributions: Conceptualisation, J.B., Y.K., Z.-W.C. and A.B.W.; methodology, J.B., Y.K., Z.-W.C. and A.B.W.; software, J.B. and Z.-W.C.; formal analysis, J.B.; writing—original draft preparation, J.B.; writing—review and editing, J.B., Y.K., Z.-W.C. and A.B.W.; supervision, Y.K., S.C. and Q.S.; project administration, Y.K.; funding acquisition, Y.K. All authors have read and agreed to the published version of the manuscript.

Funding: This research was funded by the World Meteorological Organization as part of the Climate Risk and Early Warning Systems project for Papua New Guinea (CREWS-PNG).

Data Availability Statement: GSMaP data provided by EORC, JAXA. MSWEP data provided by GloH2O. Contains modified ECMWF S2S forecast data. ENSO and IOD data sourced from the BoM.

Acknowledgments: This research was supported by the CREWS-PNG project. WMO SWCEM provided satellite-derived products, SPI and VHI. The S2S team provided gridded tercile exceedance products for the SEA5 model which were used to generate median exceedance products for the 46-day ECMWF S2S model over the study period.

Conflicts of Interest: The authors declare no conflict of interest.

Appendix A

Table A1. Mean, median and standard deviation for provincially averaged SPI-3.

Province	Provincial Mean SPI-3	Provincial Median SPI-3	Provincial SPI-3 Standard Deviation
(national— from Table 3)	0.32	0.48	0.62
Bougainville	0.20	0.23	0.77
Central	0.19	0.32	0.84
Chimbu/Simbu	0.21	0.28	0.83
East New Britain	0.55	0.73	0.67
East Sepik	0.45	0.52	0.59
Eastern Highlands	0.45	0.53	0.75
Enga	0.35	0.41	0.62
Gulf	0.11	0.25	1.01

Hela	0.14	0.36	0.95
Jiwaka	0.33	0.41	0.63
Madang	0.50	0.49	0.64
Manus	0.25	0.28	0.93
Milne Bay	0.33	0.50	0.78
Morobe	0.64	0.73	0.73
National Capital District	0.25	0.20	0.92
New Ireland	0.62	0.72	0.67
Northern Oro	0.39	0.40	0.79
Southern Highlands	0.01	0.13	1.03
West New Britain	0.45	0.55	0.74
West Sepik	0.45	0.63	0.67
Western	0.09	0.30	0.89
Western Highlands	0.37	0.41	0.67

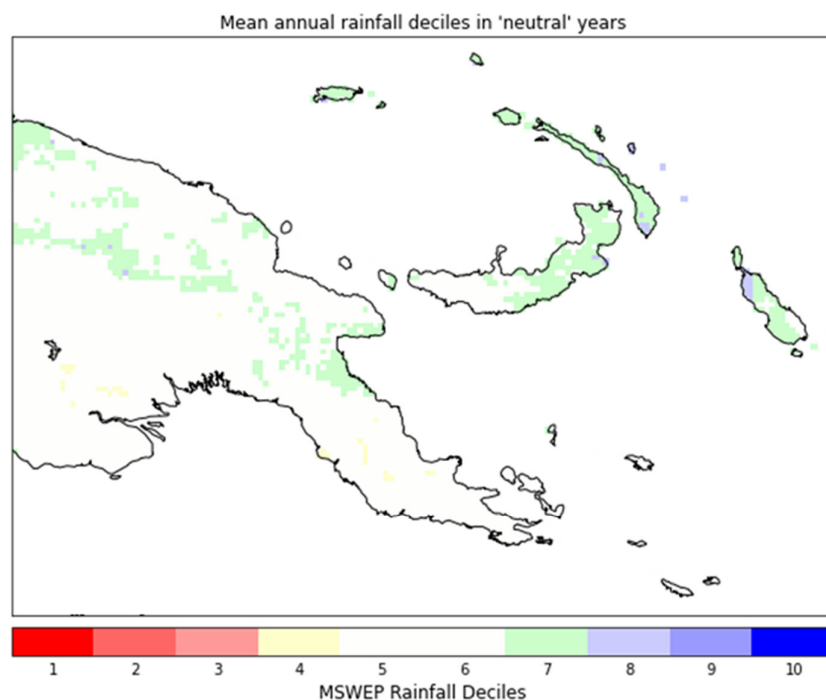
Table A2. Mean, median and standard deviation for provincially averaged VHI-3.

Province	Provincial Mean	Provincial Median	Provincial VHI-3
	VHI-3	VHI-3	Standard Deviation
(national— from Table 3)	44.63	45.55	3.21
Bougainville	42.18	42.06	2.34
Central	44.25	45.15	2.45
Chimbu/Simbu	44.79	45.42	2.70
East New Britain	42.52	42.56	1.90
East Sepik	44.54	45.22	5.10
Eastern Highlands	44.14	43.91	2.78
Enga	41.61	41.85	2.64
Gulf	43.52	43.32	3.77
Hela	42.44	42.92	1.98
Jiwaka	43.80	44.68	3.19
Madang	44.93	45.66	3.96
Manus	45.06	45.32	2.84
Milne Bay	45.55	45.70	2.75
Morobe	44.47	45.30	2.97
National Capital District	49.92	49.64	8.89
New Ireland	43.86	43.80	1.94
Northern Oro	46.59	46.94	3.64
Southern Highlands	42.90	43.27	2.18
West New Britain	43.44	43.75	1.87
West Sepik	44.44	44.90	3.27
Western	47.05	46.75	5.80
Western Highlands	45.05	45.31	3.55

Table A3. Mean, median and standard deviation for provincially averaged CEMR.

Province	Provincial Mean	Provincial Median	Provincial CEMR
	CEMR	CEMR	Standard Deviation
(national— from Table 3)	53.79	57.92	19.90
Bougainville	60.07	63.07	22.18
Central	50.22	52.90	22.82
Chimbu/Simbu	50.74	57.48	23.75
East New Britain	62.37	66.18	23.21

East Sepik	59.18	57.57	22.18
Eastern Highlands	53.62	59.92	24.15
Enga	53.50	56.39	20.67
Gulf	48.61	50.56	25.34
Hela	52.71	58.35	24.59
Jiwaka	51.66	54.86	23.46
Madang	57.35	58.28	23.63
Manus	45.93	47.86	30.67
Milne Bay	49.62	54.82	26.58
Morobe	59.17	65.10	24.13
National Capital District	46.19	47.11	23.79
New Ireland	58.04	64.33	26.64
Northern Oro	55.19	61.08	25.17
Southern Highlands	48.32	52.50	26.58
West New Britain	57.35	63.16	24.37
West Sepik	57.01	59.51	23.30
Western	49.10	53.90	28.38
Western Highlands	50.27	52.60	24.25



Base period: 1980 to 2020

Neutral years: 1980, 1984, 1985, 1986, 1990, 1993, 2001, 2003, 2004, 2005, 2008, 2009, 2013, 2017, 2018

Figure A1. MSWEP rainfall deciles in “neutral” years (ENSO and IOD inactive years).

References

1. Wilhite, D.A.; Glantz, M.H. Understanding: The Drought Phenomenon: The Role of Definitions. *Water Int.* **1985**, *10*, 111–120.
2. Iese, V.; Kiem, A.S.; Mariner, A.; Malsale, P.; Tofaeono, T.; Kirono, D.G.C.; Round, V.; Heady, C.; Tigona, R.; Veisa, F.; et al. Historical and Future Drought Impacts in the Pacific Islands and Atolls. *Clim. Change* **2021**, *166*, 19, doi:10.1007/s10584-021-03112-1.
3. Kuleshov, Y.; McGree, S.; Jones, D.; Charles, A.; Cottrill, A.; Prakash, B.; Atalifo, T.; Nihmei, S.; Seuseu, F.L.S.K. Extreme Weather and Climate Events and Their Impacts on Island Countries in the Western Pacific: Cyclones, Floods and Droughts. *Atmos. Clim. Sci.* **2014**, *4*, 803.

4. Behlert, B.; Diekjobst, R.; Felgentreff, C.; Manandhar, T.; Mucke, P.; Pries, L.; Radtke, K.; Weller, D. *The WorldRiskReport 2020*; Bündnis Entwicklung Hilft, Ruhr University Bochum—Institute for International Law of Peace and Armed Conflict (IFHV): Bochum, Germany, 2020; pp. 43–51, ISBN 978-3-946785-10-1.
5. Bourke, R.M.; Harwood, T. *Food and Agriculture in Papua New Guinea*; ANU E Press: Canberra, Australia, 2009; ISBN 1921536616.
6. Cobon, D.H.; Ewai, M.; Inape, K.; Bourke, R.M. Food Shortages Are Associated with Droughts, Floods, Frosts and ENSO in Papua New Guinea. *Agric. Syst.* **2016**, *145*, 150–164, doi:10.1016/j.agry.2016.02.012.
7. Jacka, J.K. In the Time of Frost: El Niño and the Political Ecology of Vulnerability in Papua New Guinea. *Anthropol. Forum* **2020**, *30*, 141–156, doi:10.1080/00664677.2019.1647832.
8. Nunn, P.D.; Kumar, R. Alluvial Charcoal in the Sigatoka Valley, Viti Levu Island, Fiji. *Palaeogeogr. Palaeoclimatol. Palaeoecol.* **2004**, *213*, 153–162.
9. Intergovernmental Panel on Climate Change (IPCC) The Impact of Climate Change on Natural Disasters. In *Reducing Disaster: Early Warning Systems For Climate Change*; Singh, A., Zommers, Z., Eds.; Springer Netherlands: Dordrecht, The Netherlands, 2014; pp. 21–49, ISBN 978-94-017-8598-3.
10. Wilhite, D.A. Managing Drought Risk in a Changing Climate. *Clim. Res.* **2016**, *70*, 99–102.
11. Wilhite, D.A.; Hayes, M.J.; Knutson, C.; Smith, K.H. Planning for Drought: Moving from Crisis to Risk Management. *JAWRA J. Am. Water Resour. Assoc.* **2000**, *36*, 697–710.
12. United Nations Development Programme (UNDP). *Five Approaches to Build Functional Early Warning Systems*; United Nations Development Programme: Geneva, Switzerland, 2018.
13. Kelman, I.; Glantz, M.H. Early Warning Systems Defined. In *Reducing Disaster: Early Warning Systems For Climate Change*; Singh, A., Zommers, Z., Eds.; Springer Netherlands: Dordrecht, The Netherlands, 2014; pp. 89–108, ISBN 978-94-017-8598-3.
14. World Meteorological Organization (WMO). *Multi-Hazard Early Warning Systems: A Checklist*; World Meteorological Organization: Geneva, Switzerland, 2018.
15. Merz, B.; Kuhlicke, C.; Kunz, M.; Pittore, M.; Babeyko, A.; Bresch, D.N.; Domeisen, D.I. V.; Feser, F.; Koszalka, I.; Kreibich, H.; et al. Impact Forecasting to Support Emergency Management of Natural Hazards. *Rev. Geophys.* **2020**, *58*, e2020RG000704, doi:10.1029/2020RG000704.
16. Macherera, M.; Chimbari, M.J. A Review of Studies on Community Based Early Warning Systems. *Jambá* **2016**, *8*, doi:10.4102/jamba.v8i1.206.
17. Garcia Londoño, C. Mountain Risk Management: Integrated People Centred Early Warning System as a Risk Reduction Strategy, Northern Italy. Ph.D. Thesis, University of Milano-Bicocca, Milan, Italy, 2011.
18. Baudoin, M.-A.; Henly-Shepard, S.; Fernando, N.; Sitati, A.; Zommers, Z. From Top-Down to “Community-Centric” Approaches to Early Warning Systems: Exploring Pathways to Improve Disaster Risk Reduction Through Community Participation. *Int. J. Disaster Risk Sci.* **2016**, *7*, 163–174, doi:10.1007/s13753-016-0085-6.
19. Andersson, L.; Wilk, J.; Graham, L.P.; Wikner, J.J.; Mokwatlo, S.; Petja, B. Local Early Warning Systems for Drought – Could They Add Value to Nationally Disseminated Seasonal Climate Forecasts? *Weather Clim. Extrem.* **2019**, *28*, 100241, doi:10.1016/j.wace.2019.100241.
20. Basher, R. Global Early Warning Systems for Natural Hazards: Systematic and People-Centred. *Philos. Trans. R. Soc. A Math. Phys. Eng. Sci.* **2006**, *364*, 2167–2182, doi:10.1098/rsta.2006.1819.
21. Garcia, C.; Fearnley, C. Evaluating Critical Links in Early Warning Systems. *Environ. Hazards* **2012**, *11*, 123–137, doi:10.1080/17477891.2011.609877.
22. Kuleshov, Y.; Inape, K.; Watkins, A.B.; Bear-Crozier, A.; Chua, Z.-W.; Xie, P.; Kubota, T.; Tashima, T.; Stefanski, R.; Kurino, T. Climate Risk and Early Warning Systems (CREWS) for Papua New Guinea. In *Drought (Aridity)*; IntechOpen: London, UK, 2019.
23. Bhardwaj, J.; Kuleshov, Y.; Watkins, A.; Aitkenhead, I.; Asghari, A. Building Capacity for a User-Centred Integrated Early Warning System (I-EWS) for Drought in the Northern Murray-Darling Basin. *Nat. Hazards* **2021**, *107*, 1–26, doi:10.1007/s11069-021-04575-2.
24. Svoboda, Mark D., and Brian A. Fuchs. *Handbook of Drought Indicators and Indices*; World Meteorological Organisation and Global Water Partnership: Geneva, Switzerland, 2016.
25. Gyasi-Agyei, Y. Identification of the Optimum Rain Gauge Network Density for Hydrological Modelling Based on Radar Rainfall Analysis. *Water* **2020**, *12*, 1906.
26. Michelson, D.B. Systematic Correction of Precipitation Gauge Observations Using Analyzed Meteorological Variables. *J. Hydrol.* **2004**, *290*, 161–177.
27. Kidd, C.; Shige, S.; Vila, D.; Tarnavsky, E.; Yamamoto, M.K.; Maggioni, V.; Maseko, B. The IPWG Satellite Precipitation Validation Effort. In *Satellite Precipitation Measurement*; Springer: Berlin/Heidelberg, Germany, 2020; pp. 453–470.
28. Ebert, E.E.; Janowiak, J.E.; Kidd, C. Comparison of Near-Real-Time Precipitation Estimates from Satellite Observations and Numerical Models. *Bull. Am. Meteorol. Soc.* **2007**, *88*, 47–64.
29. Du, T.L.T.; Bui, D.; Nguyen, M.D.; Lee, H. Satellite-Based, Multi-Indices for Evaluation of Agricultural Droughts in a Highly Dynamic Tropical Catchment, Central Vietnam. *Water* **2018**, *10*, 659.
30. Chua, Z.-W.; Kuleshov, Y.; Watkins, A.B. Drought Detection over Papua New Guinea Using Satellite-Derived Products. *Remote Sens.* **2020**, *12*, 3859.

31. Anshuka, A.; Buzacott, A.J. V; Vervoort, R.W.; van Ogtrop, F.F. Developing Drought Index–Based Forecasts for Tropical Climates Using Wavelet Neural Network: An Application in Fiji. *Theor. Appl. Climatol.* **2021**, *143*, 557–569, doi:10.1007/s00704-020-03446-3.
32. Han, P.; Wang, P.X.; Zhang, S.Y. Drought Forecasting Based on the Remote Sensing Data Using ARIMA Models. *Math. Comput. Model.* **2010**, *51*, 1398–1403.
33. Rhee, J.; Im, J.; Park, S.; Forest, R. Drought Forecasting Based on Machine Learning of Remote Sensing and Long-Range Forecast Data. *APEC Clim. Cent. Repub. Korea* **2016**, doi:10.5194/isprs-archives-XLI-B8-157-2016.
34. Yan, H.; Moradkhani, H.; Zarekarizi, M. A Probabilistic Drought Forecasting Framework: A Combined Dynamical and Statistical Approach. *J. Hydrol.* **2017**, *548*, 291–304.
35. Hao, Z.; Singh, V.P.; Xia, Y. Seasonal Drought Prediction: Advances, Challenges, and Future Prospects. *Rev. Geophys.* **2018**, *56*, 108–141.
36. Steinemann, A.C. Using Climate Forecasts for Drought Management. *J. Appl. Meteorol. Climatol.* **2006**, *45*, 1353–1361.
37. United Nations Office for Disaster Risk Reduction (UNDRR). *Disaster Risk Reduction in Papua New Guinea: Status Report 2019*; United Nations Office for Disaster Risk Reduction, Bangkok, Thailand, 2019.
38. Centre for Excellence in Disaster Management & Humanitarian Assistance. *Papua New Guinea Disaster Management Reference Handbook*; Centre for Excellence in Disaster Management & Humanitarian Assistance: Joint Base Pearl Harbor-Hickam, HI, USA, 2019.
39. National Geophysical Data Center, NESDIS, NOAA, US Department Commerce. *NOAA National Geophysical Data Center ETOPO1 1 Arc-Minute Global Relief Model*; National Geophysical Data Center, NESDIS, NOAA, US Department Commerce: Boulder, CO, USA, 2009; doi:10.7289/V5C8276M.
40. Benjamin, A.K.; Mopafi, I.; Duke, T. A Perspective on Food and Nutrition in the PNG Highlands. *Food Secur. Papua New Guinea* **2001**, *11*, 94.
41. Lutulele, R.P. Sweet Potato Variety Developments in the PNG Highlands: Implications for Future Research and Extension Focus. In Proceedings of the Food Security for Papua New Guinea Proceedings of the Papua New Guinea Food and Nutrition 2000 Conference (ACIAR Proceedings 99) University of Technology, Lae, Papua New Guinea, 26–30 June 2001; pp. 683–688.
42. Prentice, M.L.; Hope, G.S. Climate of Papua. *Ecol. Papua* **2007**, *1*, 479–494.
43. Beck, H.; Zimmermann, N.; McVicar, T.; Vergopolan, N.; Berg, A.; Wood, E. Present and Future Köppen–Geiger Climate Classification Maps at 1-Km Resolution. *Sci. Data* **2018**, *5*, 180214, doi:10.1038/sdata.2018.214.
44. Smith, I.; Moise, A.; Inape, K.; Murphy, B.; Colman, R.; Power, S.; Chung, C. ENSO-Related Rainfall Changes over the New Guinea Region. *J. Geophys. Res. Atmos.* **2013**, *118*, 10,610–665,675, doi:https://doi.org/10.1002/jgrd.50818.
45. Gressit, J.L. *Biogeography and Ecology of New Guinea*; Springer Science & Business Media: Berlin/Heidelberg, Germany, 2012; Volume 42, ISBN 9400986327.
46. Park, S.-Y.; Sur, C.; Kim, J.-S.; Lee, J.-H. Evaluation of Multi-Sensor Satellite Data for Monitoring Different Drought Impacts. *Stoch. Environ. Res. Risk Assess.* **2018**, *32*, 2551–2563.
47. Choi, M.; Jacobs, J.M.; Anderson, M.C.; Bosch, D.D. Evaluation of Drought Indices via Remotely Sensed Data with Hydrological Variables. *J. Hydrol.* **2013**, *476*, 265–273, doi:10.1016/j.jhydrol.2012.10.042.
48. Halwatura, D.; McIntyre, N.; Lechner, A.M.; Arnold, S. Capability of Meteorological Drought Indices for Detecting Soil Moisture Droughts. *J. Hydrol. Reg. Stud.* **2017**, *12*, 396–412.
49. McKee, T.B. Drought Monitoring with Multiple Time Scales. In Proceedings of the 9th Conference on Applied Climatology, Boston, MA, USA, January 15–20 1995.
50. Kogan, F.N. Global Drought Watch from Space. *Bull. Am. Meteorol. Soc.* **1997**, *78*, 621–636, doi:10.1175/1520-0477(1997)078<0621:GDWFS>2.0.CO;2.
51. Vitart, F. Evolution of ECMWF Sub-Seasonal Forecast Skill Scores. *Q. J. R. Meteorol. Soc.* **2014**, *140*, 1889–1899, doi:https://doi.org/10.1002/qj.2256.
52. European Centre for Medium-Range Weather Forecasts (ECMWF) S2S, ECMWF, Realtime, Instantaneous and Accumulated Available online: <https://apps.ecmwf.int/datasets/data/s2s-realtime-instantaneous-accum-ecmf/levtype=sfc/type=pf/> (accessed on 17 June 2021).
53. Kuleshov, Y.; Kurino, T.; Kubota, T.; Tashima, T.; Xie, P. WMO Space-Based Weather and Climate Extremes Monitoring Demonstration Project (SEMMP): First Outcomes of Regional Cooperation on Drought and Heavy Precipitation Monitoring for Australia and Southeast Asia; IntechOpen: London, UK 2019, ISBN 978-1-78984-734-5.
54. Beck, H.E.; Wood, E.F.; Pan, M.; Fisher, C.K.; Miralles, D.G.; Van Dijk, A.I.J.M.; McVicar, T.R.; Adler, R.F. MSWEP V2 Global 3-Hourly 0.1 Precipitation: Methodology and Quantitative Assessment. *Bull. Am. Meteorol. Soc.* **2019**, *100*, 473–500.
55. Kubota, T.; Aonashi, K.; Ushio, T.; Shige, S.; Takayabu, Y.N.; Kachi, M.; Arai, Y.; Tashima, T.; Masaki, T.; Kawamoto, N. Global Satellite Mapping of Precipitation (GSMaP) products in the GPM era. In *Satellite Precipitation Measurement*; Springer: Berlin/Heidelberg, Germany, 2020; pp. 355–373.
56. Aonashi, K.; Awaka, J.; Hirose, M.; Kozu, T.; Kubota, T.; Liu, G.; Shige, S.; Kida, S.; Seto, S.; Takahashi, N.; et al. GSMaP Passive Microwave Precipitation Retrieval Algorithm: Algorithm Description and Validation. *J. Meteorol. Soc. Japan. Ser. II* **2009**, *87A*, 119–136, doi:10.2151/jmsj.87A.119.
57. Bureau of Meteorology ENSO Outlook History. Available online: <http://www.bom.gov.au/climate/enso/outlook/#tabs=ENSO-Outlook-history> (accessed on 16 August 2021).

58. Murphy, B.F.; Power, S.B.; McGree, S. The Varied Impacts of El Niño–Southern Oscillation on Pacific Island Climates. *J. Clim.* **2014**, *27*, 4015–4036.
59. Bureau of Meteorology ENSO History—La Niña Impacts Available online: <http://www.bom.gov.au/climate/enso/#tabs=Pacific-Ocean&pacific=History&enso-impacts=La-Niña-impacts> (accessed on 16 August 2021).
60. Bureau of Meteorology ENSO History—El Niño Impacts Available online: <http://www.bom.gov.au/climate/enso/#tabs=Pacific-Ocean&pacific=History&enso-impacts=El-Niño-impacts> (accessed on 16 August 2021).
61. Bureau of Meteorology Indian Ocean History Available online: <http://www.bom.gov.au/climate/enso/#tabs=Indian-Ocean&indian=History> (accessed on 16 August 2021).
62. Bureau of Meteorology Indian and Pacific Ocean Interaction History Available online: <http://www.bom.gov.au/climate/enso/#tabs=Indian-Ocean&indian=History&iod-impacts=Pacific-Ocean-interaction> (accessed on 16 August 2021).
63. Dinku, T.; Ceccato, P.; Grover-Kopec, E.; Lemma, M.; Connor, S.J.; Ropelewski, C.F. Validation of Satellite Rainfall Products over East Africa’s Complex Topography. *Int. J. Remote Sens.* **2007**, *28*, 1503–1526.
64. Deo, R.C. On Meteorological Droughts in Tropical Pacific Islands: Time-series Analysis of Observed Rainfall Using Fiji as a Case Study. *Meteorol. Appl.* **2011**, *18*, 171–180.
65. Sufri, S.; Dwirahmadi, F.; Phung, D.; Rutherford, S. A Systematic Review of Community Engagement (CE) in Disaster Early Warning Systems (EWSs). *Prog. Disaster Sci.* **2020**, *5*, 100058, doi:10.1016/j.pdisas.2019.100058.
66. Barrett, A.B.; Duivenvoorden, S.; Salakpi, E.E.; Muthoka, J.M.; Mwangi, J.; Oliver, S.; Rowhani, P. Forecasting Vegetation Condition for Drought Early Warning Systems in Pastoral Communities in Kenya. *Remote Sens. Environ.* **2020**, *248*, 111886, doi:<https://doi.org/10.1016/j.rse.2020.111886>.
67. Zhu, Y.; Wang, W.; Singh, V.P.; Liu, Y. Combined Use of Meteorological Drought Indices at Multi-Time Scales for Improving Hydrological Drought Detection. *Sci. Total Environ.* **2016**, *571*, 1058–1068, doi:10.1016/j.scitotenv.2016.07.096.
68. Ji, T.; Li, G.; Yang, H.; Liu, R.; He, T. Comprehensive Drought Index as an Indicator for Use in Drought Monitoring Integrating Multi-Source Remote Sensing Data: A Case Study Covering the Sichuan-Chongqing Region. *Int. J. Remote Sens.* **2018**, *39*, 786–809.
69. Krishnamurthy R, P.K.; Fisher, J.B.; Schimel, D.S.; Kareiva, P.M. Applying Tipping Point Theory to Remote Sensing Science to Improve Early Warning Drought Signals for Food Security. *Earth’s Futur.* **2020**, *8*, e2019EF001456, doi:10.1029/2019EF001456.
70. Lavaysse, C.; Vogt, J.; Pappenberger, F. Early Warning of Drought in Europe Using the Monthly Ensemble System from ECMWF. *Hydrol. Earth Syst. Sci.* **2015**, *19*, 3273–3286.
71. Hoover, J.D.; Leisz, S.J.; Laituri, M.E. Comparing and Combining Landsat Satellite Imagery and Participatory Data to Assess Land-Use and Land-Cover Changes in a Coastal Village in Papua New Guinea. *Hum. Ecol.* **2017**, *45*, 251–264.
72. Tsakiris, G.; Vangelis, H. Towards a Drought Watch System Based on Spatial SPI. *Water Resour. Manag.* **2004**, *18*, 1–12.
73. White, J.; Fu, K.-W. Who Do You Trust? Comparing People-Centered Communications in Disaster Situations in the United States and China. *J. Comp. Policy Anal. Res. Pract.* **2012**, *14*, 126–142, doi:10.1080/13876988.2012.664688.
74. Xue, K.; Guo, S.; Liu, Y.; Liu, S.; Xu, D. Social Networks, Trust, and Disaster-Risk Perceptions of Rural Residents in a Multi-Disaster Environment: Evidence from Sichuan, China. *Int. J. Environ. Res. Public Health* **2021**, *18*, doi:10.3390/ijerph18042106.
75. Goniewicz, K.; Burkle, F. Disaster Early Warning Systems: The Potential Role and Limitations of Emerging Text and Data Messaging Mitigation Capabilities. *Disaster Med. Public Health Prep.* **2019**, *13*, doi:10.1017/dmp.2018.171.
76. Cambers, G.; Carruthers, P.; Rabuatoka, T.; Tubuna, S.; Ungaro, J. Implementing Climate Change Adaptation Interventions in Remote Outer Islands of the Pacific Island Region. In *Climate Change Adaptation in Pacific Countries: Fostering Resilience and Improving the Quality of Life*; Leal Filho, W., Ed.; Springer International Publishing: Cham, Switzerland, 2017; pp. 3–18, ISBN 978-3-319-50094-2.
77. Griffen, V. Gender Relations in Pacific Cultures and Their Impact on the Growth and Development of Children. In Proceedings of the Children’s Rights and Culture in the Pacific Seminar, 30 October 2006. Available online: http://linkasea.pbworks.com/f/Griffen+Gender_Relations_in_Pacific_cultures.pdf (accessed on 17 August 2021).
78. Clissold, R.; Westoby, R.; McNamara, K.E. Women as Recovery Enablers in the Face of Disasters in Vanuatu. *Geoforum* **2020**, *113*, 101–110, doi:10.1016/j.geoforum.2020.05.003.
79. Morioka, K.; Aid, A. A Climate for Change: Understanding Women’s Vulnerability and Adaptive Capacity to Climate Change from ActionAid’s Rights-Based Approach-Case Studies from Papua New Guinea and Solomon Islands; Sydney, Australia, 2012. Available online: https://reliefweb.int/sites/reliefweb.int/files/resources/a%20climate%20for%20change_final.pdf (accessed on 17 August 2021).
80. Aipira, C.; Kidd, A.; Morioka, K. *Climate Change Adaptation in Pacific Countries: Fostering Resilience Through Gender Equality*; Springer, Cham, Denmark, 2017; pp. 225–239, ISBN 978-3-319-50093-5.
81. Campbell, J.R. *Traditional Disaster Reduction in Pacific Island Communities*; GNS Science: Institute of Geological and Nuclear Sciences Ltd.: Wellington, New Zealand, 2006; ISBN 0478099614.
82. Nalau, J.; Handmer, J.; Dalesa, M. The Role and Capacity of Government in a Climate Crisis: Cyclone Pam in Vanuatu. In *Climate Change Adaptation in Pacific Countries: Fostering Resilience and Improving the Quality of Life*; Leal Filho, W., Ed.; Springer International Publishing: Cham, Switzerland, 2017; pp. 151–161, ISBN 978-3-319-50094-2.

-
83. Mercer, J.; Kelman, I.; Suchet-pearson, S.; Lloyd, K. Integrating Indigenous and Scientific Knowledge Bases for Disaster Risk Reduction in Papua New Guinea. *Geogr. Ann. Ser. B Hum. Geogr.* **2009**, *91*, 157–183, doi:10.1111/j.1468-0467.2009.00312.x.
 84. Mercer, J.; Kelman, I.; Taranis, L.; Suchet-Pearson, S. Framework for Integrating Indigenous and Scientific Knowledge for Disaster Risk Reduction. *Disasters* **2010**, *34*, 214–239, doi:10.1111/j.1467-7717.2009.01126.x.